XIII ICSMFE, 1994, New Delhi, India / XIII CIMSTF, 1994, New Delhi, Inde

BACK ANALYSIS OF BACKFILL COMPACTED RETAINING WALL CASE HISTORIES

ETUDE RETROSPECTIVE DES CAS TYPES DE MURS DE SOUTIEN COMPACTES AU MOYEN DE REMBLAIS

S.A.S. Kulathilaka

Department of Civil Engineering
University of Moratuwa, Moratuwa, Sri Lanka

Synopsis

In most instances backfill behind retaining walls needs to be compacted to satisfy serviceability criteria. Conventional earth pressure theories do not account for the compaction effects. A model is developed using an analogy between loading/unloading in the compaction process and cyclic K_o loading/unloading. The model is incorporated with an Elastic-Ideally Plastic FE model to numerically simulate the backfilling and compaction behind retaining walls. Capability of the model is assessed by application to several instrumented retaining walls and by comparing the observations made with the predictions from the numerical formulation.

1. INTRODUCTION

Often the fill area acquired by building of a earth retaining structure will be used for some purpose such as a roadway. To minimise the deformations occurring in the backfill while it is in its intended use, fill behind the retaining structure needs to be compacted. This backfill compaction applied during the incremental filling introduces additional stresses on the wall. The classical theories of Rankine and Coulomb do not account for these compaction effects, but Broms (1971), Ingold (1979) and Seed and Duncan(1983) have proposed various theories to account for them.

The numerical model developed in this research (Kulathilaka(1990) simulates the incremental filling and compaction process and computes the residual stresses induced by the compaction process. The model is incorporated with an elastic- ideally plastic FE program and the wall movements imposed by the compaction induced forces and the subsequent stress rearrangements are computed. By closely simulating the complete backfilling and compaction process, wall and soil deformations and the lateral stress distribution behind the wall are computed. This paper presents the comparison of lateral stress distributions derived through the model, with the experimental observations for a large scale experimental wall set up and one instrumented actual retaining wall. Experimental observations and model predictions are in very good agreement.

2. COMPACTION SIMULATION MODEL

2.1 Quantification of the Compaction Effort

Compaction effort applied at the surface by the plant is simulated by application of a lateral stress profile at the current surface level. In practice, compaction plant will not be taken right up to the wall. A certain minimum distance is kept between the wall surface and the edge of the compactor. Typical compactor imposed lateral stress profiles computed "near the wall" and "away from the wall in the free field" having taken the above fact into consideration will be as depicted in Figure 4 (a) and (b) respectively. The model interpolates the compactor imposed lateral stress $\Delta\sigma_{x,c}$ for the soil element under consideration using the depth to the Gauss points of the element.

2.2. Loading of an Element due to the Compactor

Prior to the present compaction increment the lateral stress level of a typical soil element in the backfill will be in a K_o state (A_1), higher than K_o state (A_2) or lower than K_o state (A_3) as in Figure 1.

If the initial stress state of the element is either K_o or lower than K_o, lateral stress and vertical stress will increase in a path parallel to the K_o line, while the compactor is still on the surface. If the initial stress state is higher than K_o, stress increase will follow a path of slope K_3 till it meets the K_o line and follow the K_o line thereafter.

Four noded isoparametric elements with four Gauss points are employed in the Finite Element formulation. Each Gauss point of an element is considered separately in the compaction simulation subroutine. Compactor imposed lateral stress increase $\Delta\sigma_{x,c}$ is interpolated depending on the depth from the surface. When the stress state is K_o or lower, the lateral stress will increase by $\Delta\sigma_{x,c}$ while the compactor is still on the surface. When the initial stress state is higher than K_o lateral stress increase will be smaller due to the initially stiffer response. This is implemented by computing an "equivalent vertical driving stress" $\Delta\sigma_v = \Delta\sigma_{x,c}/K_o$ (Figure 1).

The compaction model identifies the present stress state in the Gauss point under consideration and takes it along the appropriate stress path. Various numerical procedures are employed to capture the turning points and to implement the stress path.

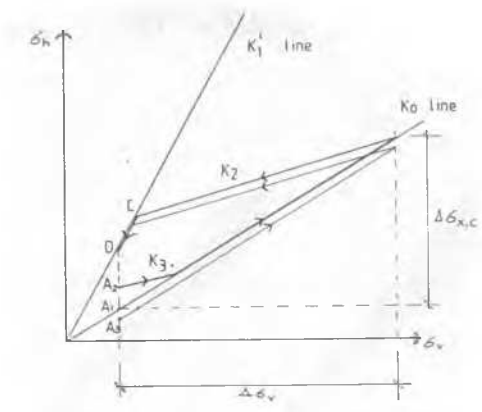

Figure 1 - Compaction Simulation Model

2. 3. Unloading due to the Removal of the Compactor

Stress release in both the vertical and horizontal directions will take place along the K_2 line during the removal of the compactor. If the unloading path meets the K_1' line prior to the reduction of the vertical stress to the overburden value, unloading will follow the K_1' line thereafter. Thus an unloading path of the form "B-C-D" will be followed. Certain numerical techniques are employed to capture the point C and to impose the path CD. The residual stress increase at the end of the compaction process is denoted by $\Delta\sigma_{x,r}$.

2 .4 Compaction Induced Forces on the Wall

By taking the Gauss points of a soil element through the compaction simulation model residual lateral stress increases are computed. The contribution to the lateral force on the wall from a soil element adjacent to the wall is computed by averaging the residual lateral stress increases.

By taking all the soil elements through the model the nodal force vector on the wall for the FE computation can be assembled.

2.5 Simulation of the Compaction Effort by a Single Increment

When the soil fill is compacted at a certain elevation, the compactor will pass a number of times over the current surface. This will cause residual stress increases in the soil and the forces thus induced on the wall will cause wall movements and stress relaxation. Nonetheless, ongoing compaction will reintroduce some of the relaxed stresses. The influence of surficial compaction in regaining these lateral stresses diminishes with the depth.

An "effective depth of compaction Effort" above which soil is expected to regain the lateral stresses relaxed due to the wall movement,is computed through a numerical procedure

For this purposes lateral stress is separated into two parts as Geostatic stress and compaction induced stress. The compaction induced stress component is obtained by accumulation of the residual stress increases in the soil element over the compaction increments. i. e.

$$\sigma_{x,comp} = \sum_{increments} \Delta\sigma_{x,r}$$
$$\sigma_{x,geo} = \sigma_x - \sigma_{x,comp}$$

If the geostatic stress component is greater than the "Compactor imposed lateral stress $\Delta\sigma_{x,c}$ " for the element in the current compaction increment, soil element is said to be below the "effective depth of compaction effort".

3. FINITE ELEMENT COMPUTATION

The FE model employed in this analysis is based on an Elastic-Ideally Plastic formulation. Finite element simulation of backfilling and compaction behind retaining walls consist of two types of load increments, namely; Placement increments (wall or soil), and Compaction increments.

For the placement increments " dense liquid technique " is employed. For the compaction increments, forces due to compaction induced stresses are computed and assembled as described above. The finite element model computes the deformations in the soil due to the applied system of forces and also computes the subsequent stress rearrangements.

However in both types of load increments lateral stress increases in the already compacted elements are governed by the compaction simulation model. In the soil elements below the effective depth of compaction, lateral stress relaxation computed by the FE model is applied.

4. APPLICATION OF THE MODEL TO BACK ANALYSE TRRL WALL - UK

A detailed description of this experimental set-up is given in Carder et al (1977). This is one of the best documented and best monitored experiments available. Set-Up depicted in Figure 2 comprises of a metal retaining wall consisting of three 2m X 2m metal panels making it a 2m high 6m wide wall and a 1 m thick concrete wall on the opposite side. All the measurements were made in the central section. Backfilling and compaction were done in a manner very similar to that in an actual field situation. In this research separate Finite element back analyses were performed on the concrete wall and the metal wall.

4.1 Metal Retaining Wall

4.1.1 General

The Finite Element mesh used to idealise the metal wall is depicted in Figure 3. In accordance with the neutral axis defined by Carder et al (1977) through the centerline of the set-up, a soil continuum extending up to the defined neutral axis is descretised for the FE study. At the nodes along the vertical boundary at the neutral axis, only vertical movements were allowed. The soil mass was divided in to 127 plane strain elements.

Metal retaining wall was modelled by eight beam elements. Due to the smaller thickness of the wall, it is observed that modelling the wall by plane strain elements would give it an unrealistic rigidity and would not model the flexural nature of the wall. The two jack support system to the wall was modelled as spring support conditions.

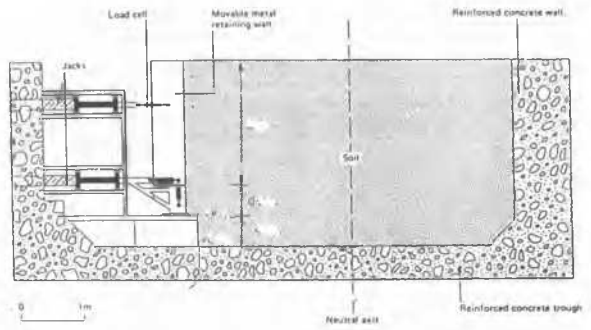

Figure 2 - TRRL Experimental Wall Set up (After Carder et al 1977)

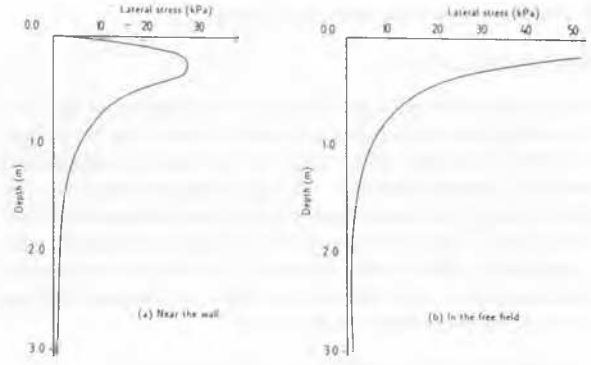

Figure 4 - Compactor Imposed Lateral Stress Profiles - TRRL Wall

All the nodes at the base of the set up on the concrete floor were assumed to be restrained. The nodes on the left boundary up to the level of the base of the metal wall were also restrained. There will be a relative movement between the sand backfill and the vertical concrete boundary and also between the metal wall and the backfill, during the backfilling and compaction process. This was accurately modelled by deploying one dimensional joint elements along those boundaries as depicted in Figure 3.

4.1.2 Simulation of backfilling and compaction

In the experiment soil was placed in 0.20m thick layers. F E mesh used in this study element layers are of thickness 0.25m. Thus the soil is modelled to have placed and compacted in 0.25m thick layers. This is not expected to cause any significant difference.

The soil was compacted by six passes of a 1.3 tonne twin roll vibrating roller. The quantified profiles of "Compactor imposed lateral pressures " are shown in Figure 4. These profiles are applied at the surface level of each layer during the incremental compaction. The closest the roller came to the retaining wall was a distance of 0.15m. The compactor induced lateral stress profiles were accordingly computed.

Incremental placement of layers and their compaction was simulated as described in section 2.

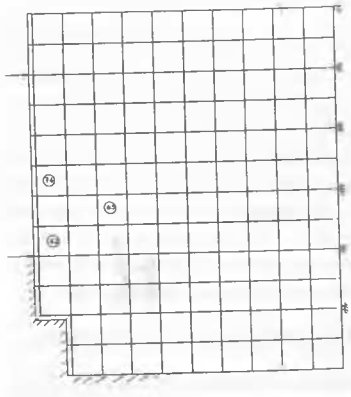

Figure 3 - FE Mesh - TRRL Metal Retaining Wall

4. 1. 3. Observations and discussion

The final lateral stress profile on the metal retaining wall computed using the above numerical process is presented in Figure 5 (a). Also the average lateral stress profile observed by Carder et al (1977) in their first experiment is presented in the same diagram. It can be seen that the values predicted by the numerical model are in excellent agreement with the experimental observations. Towards the deeper levels the relaxation of the lateral stress due to the deformations is also notable. It is also evident that the lateral stresses computed are much greater than the K_o values over the whole depth.

Carder et al(1977) presented the displacements at wall nodes in the form of, "the displacement at each level of the wall from the stage when soil was first compacted at that level until compaction to the full height was complete". The corresponding displacements at the wall nodes were evaluated in this numerical study, using the cumulative displacements at various stages. The comparison of computed displacements with the Carder et al(1977) experimental observations is depicted in Figure 5 (b). The numerical results and the observations are in very good agreement, over the full depth of the wall.

The case of the incremental building up of the backfill without compaction was also studied. Figure 5(c) compares the lateral stress profile computed for this case with the one obtained for the compacted backfill. The higher lateral stresses generated in the compacted backfill are quite evident.

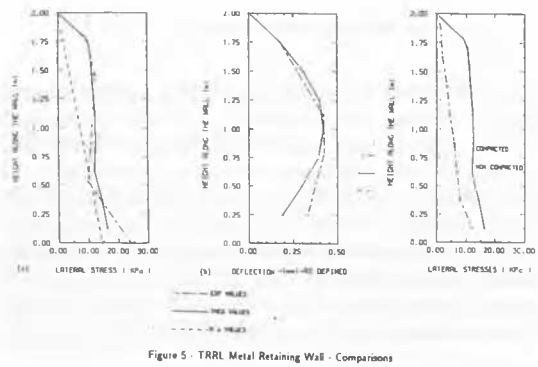

Figure 5 - TRRL Metal Retaining Wall - Comparisons

4. 2 TRRL - Concrete Retaining Wall

4.2.1 General

The finite element mesh used to study the behaviour of the concrete retaining wall is as shown in Figure 6. In this case the continuum used for the study was extended further than the neutral axis defined by Carder et al(1977). The rigid concrete base was also modelled using plane strain elements and exact shape of the wall was considered. The thick concrete wall and soil elements were also modelled as plane strain elements. To allow for the relative displacement between the backfill and the rigid concrete wall one dimensional interface elements were used.

4.2.2 Simulation of backfilling and compaction

Being in the same set-up the backfill placement and compaction procedure was the same as that for the metal retaining wall.Therefo in the numerical simulation process the same procedures as for the metal retaining wall were adopted and the same compactor imposed lateral stress profiles were used.

4. 2. 3 Observations and discussion

The final lateral stress profile acting on the concrete retaining wall computed using the numerical model is depicted in Figure 7 (a). The lateral stress measurements made by Carder et al(1977) are also presented in the same Figure. The computed values are seen to be in very good agreement with the experimental observations. The differences between the observed and computed values are smaller than the scatter within the observations themselves. Also the lateral stress values are somewhat higher than for the more flexible metal retaining wall.

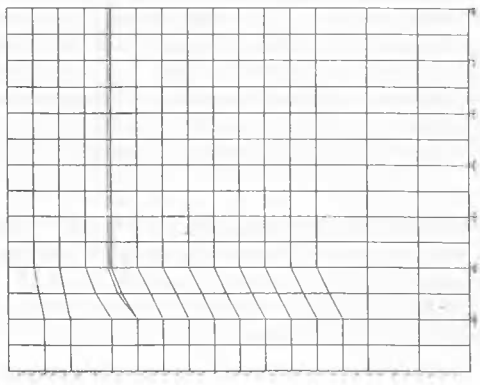

Figure 6 - FE Mesh - TRRL Concrete Retaining Wall

Over the top 2m depth of the wall, the lateral stresses are much larger than K_o values. Over the lower 1m depth the compacted profile is only slightly larger than the K_o values. Similar observations were made with the Broms(1971) and Ingold(1979) theories. When the wall is tall enough, beyond a certain depth lateral stresses were around K_o values. This in fact is an illustration of the diminishing influence of the surficial compaction on these lower layers (Metal retaining wall was only 2m deep and thus a similar behaviour was not exhibited.) Any rotation of the wall, leading to a lateral stress increase near the toe was inhibited by the concrete trough.

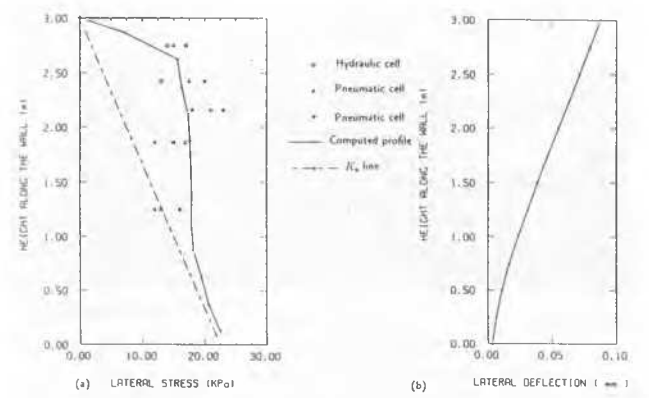

Figure 7 - TRRL Concrete Retaing Wall - Comparisons

The deflections of the wall were also computed and the final deflected shape of the wall is shown in Figure 7 (b). The maximum total deflection at the top of the wall is found to be less than 0.1mm. This justifies the Carder et al assumption of the wall to be rigid.Also because of this rigidity no relaxation of stress will occur due to the deflection of the wall, and this resulted in much higher stresses than for the metal wall.

5. CONCRETE RETAINING WALL SUPPORTING A HIGHWAY IN TEXAS

5.1 General

The experimental observations made by Coyle et al (1974) on a concrete retaining wall supporting a highway in Texas were used in the third case study. This is of special interest because it is a retaining wall used in real practice and it has different foundation conditions. This wall was constructed on a strip footing resting on steel piles and the space between the existing embankment and the wall is filled up with a cohesionless soil. A comprehensive review of the experimental procedure and the the results were presented in Coyle et al (1974).

All the elements in the continuum are modelled as plane strain elements. It was attempted to keep the aspect ratio close to unity. To allow for the relative displacement between the wall and the soil backfill one dimensional interface elements were used.

Figure 8 depicts the actual configuration of the footing and the existing clay embankment. The finite element mesh used for the numerical analysis is shown in Figure 9. The shaded elements, below the footing level and in the embankment were assumed to exist prior to the backfilling. The water table was found to be well below the footing level. Therefore any complication due to a pore water pressure development in the clay embankment due to compaction, was avoided. As the piles were also modelled to be of concrete, their dimensions were modified to have an equivalent rigidity when treated as a continuous insitu wall.

5.2 Simulation of Backfilling and Compaction

During the filling operation the space in between the wall and the existing embankment was filled to a height of about 2m within the first two days and left for about four days. Thereafter it was filled up to the top level in two days.

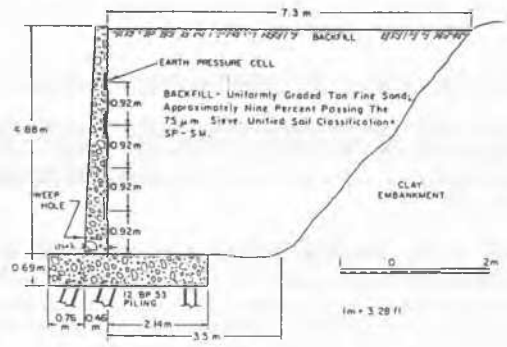

Figure 8 - Cantlever Retaining Wall Set up (Coyle et al)

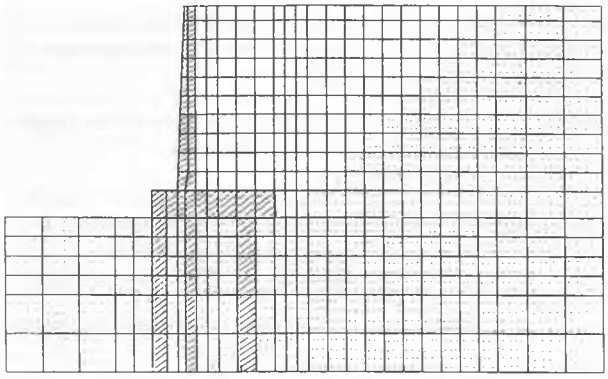

Figure 9 - FE Mesh - Coyle et al Cantilevered Wall

In the numerical simulation it was assumed to be placed in 0.5m thick layers, throughout the filling operation. In the absence of exact details of the compaction effort used some reasonable "Compactor induced stress profile" had to be assumed. Backfill was a fine silty sand with an angle of friction of 32°.

5.2.1 Compactor Imposed Lateral Stress Profiles

The concrete footing which supports the wall extends about 2.14m from the face of the wall. As this footing is supported by piles it imposes almost rigid conditions near the wall base. This footing would act as a rigid base during the compaction of the fill near the wall. Therefore the compactor-imposed lateral stress profile closer to the wall were modified to cater for these conditions.

At different fill elevations appropriately modified different induced lateral stress profiles were used. At distances further away from the footing no modifications were made. Figure 10 (a) shows a typical unmodified lateral stress profile. Figures 10 (b), (c) and (d) show some of the modified compactor induced lateral stress profiles for different fill elevations.

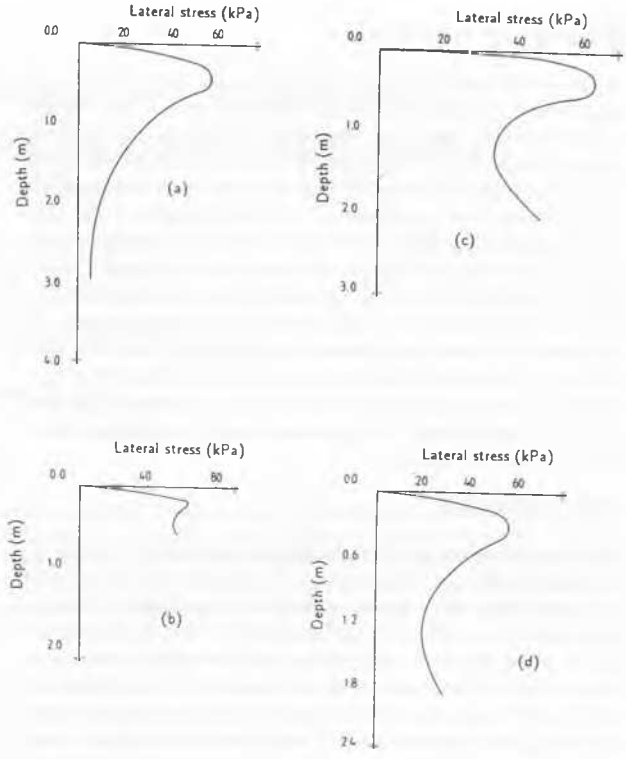

Figure 10 - Compactor Imposed Lateral Stress Profiles - Coyle et al Wall

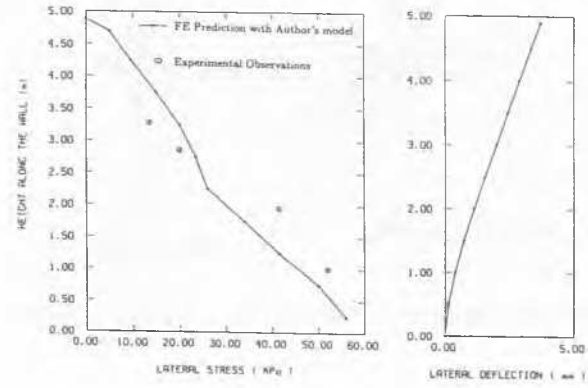

Figure 11 - Coyle et at Cantilevered Wall - Comparisons

5.3 Observations and Discussion

5.3.1 Lateral stress observations

The lateral stress distribution on the reinforced concrete wall computed by the numerical model at the end of backfilling and compaction to the top level, is presented in Figure 11 (a). The observed lateral stress values at the corresponding time were extracted from the plot of lateral stress vs time from Coyle et al (1974) and are also plotted in the same diagram. They are in very good qualitative agreement over the whole depth of the wall and a very good quantitative agreement also prevails over the most part of the wall.

5.3.2 Deflection observations

The computed lateral deflection profiles at the end of the backfilling and compaction are shown in Figure 11 (b). These values were much smaller than those reported by Coyle et al (1974) at the end of seven days. This could be attributed to the observed outward movement of 5mm of the footing, said to have caused by the heavy compaction equipment. In this back analysis, concrete piles were assumed to extend upto the base of the continuum and the footing was monolithically connected with the piles. Rigid conditions thus introduced prevented any such lateral movement. The computed movements at the footing level were negligible. If the difference of deflections between the second and seventh day are compared with the computed values much closer agreement is obtained. Nonetheless, Coyle et al (1974) have admitted that due to the disturbance caused by the construction, the displacements observed may not be accurate.

5. CONCLUSIONS

By combining the compaction simulation algorithm with the finite element stress analysis program, backfilling and compaction behind a retaining wall can be numerically simulated. The numerical model is used here to back analyse two well instrumented actual size retaining walls. Backfilling and compaction procedures adopted in the field and structural configurations were closely simulated. Backfill compaction has increase the lateral stresses on the wall from a non-compacted case. Lateral stress profiles and wall deflections computed by the model are in very good agreement with the observations made in the field.

References

1. BROMS, B. 1971 Lateral Earth Pressures due to Compaction of Cohesionless Soils. *Proceedings, 4th European Conference on Soil Mechanics and Foundation Engineering, Budapest, pp. 373-384*

2. CARDER, D. R., POLOCK, R. G., AND MURRAY, R. T. 1977 Experimental Retaining Wall Facility - Lateral Stress Measurements Wit a Sand Backfill *TRRL Laboratory Report Number 766*

3. COYLE, H. M., BARTOSWITZ, R. E., MILBERGER, L. J. AND BUTLER, H. D. 1974 Field Measurement of Lateral Earth Pressure on a Cantilever Retaining Wall. *Transportation Research Record 517, pp 16-29*

4. KULATHILAKA, S. A. S. 1990 Finite Element Analysis of Earth Retaining Structures. *Ph. D. Thesis submitted to Monash University, Australia*

5. INGOLD, T. S. 1979 The Effect of Compaction on Retaining Walls *Geótechnique 29, No. 3, pp. 265-283.*

6. SEED, R. B. AND DUNCAN, J. M. 1983 Soil-Structure Interaction Effects of Compaction Induced Stresses and Deflections. *Geotechnical Engineering Research Report No. UCB/GT/83-06, University of California, Berkeley, U.S.A.*